Tof1p Regulates DNA Damage Responses During S Phase in *Saccharomyces cerevisiae*

Eric J. Foss

Division of Basic Sciences, Fred Hutchinson Cancer Research Center, Seattle, Washington 98109-1024

Manuscript received August 7, 2000
Accepted for publication November 10, 2000

ABSTRACT

A *tof1* mutant was recovered in a screen aimed at identifying genes involved specifically in the S phase branch of the *MEC1*-dependent DNA damage response pathway. The screen was based on the observation that mutants missing this branch are particularly dependent on the cell cycle-wide branch and, therefore, on *RAD9*, for surviving DNA damage. *tof1* and *rad9* conferred synergistic sensitivity to MMS, UV, and HU, and the double mutant was incapable of slowing S phase in response to MMS, inducing *RNR3* transcription in response to UV, and phosphorylating Rad53p in response to HU. *TOF1*'s contribution to DNA damage response appeared to be restricted to S phase, since *TOF1* did not contribute to UV-induced transcription during G1 or to the *cdc13-1*-induced block to anaphase in G2/M. I suggest a model in which Tof1p functions to link Mec1p with Rad53p.

WHEN yeast cells are treated with agents that damage DNA or block DNA replication, they delay bud emergence (Siede *et al.* 1993, 1994), delay anaphase (Weinert and Hartwell 1988), slow DNA replication (Paulovich and Hartwell 1995), phosphorylate specific proteins (Sanchez *et al.* 1996; Sun *et al.* 1996; Longhese *et al.* 1997; Emili 1998), and increase transcription of specific genes (Zhou and Elledge 1993; Aboussekhra *et al.* 1996; Kiser and Weinert 1996). These responses are frequently called "checkpoint" responses. The pathway that regulates these responses contains two branches, one of which functions throughout the cell cycle (referred to here as the cell cycle-wide pathway) and one of which functions specifically during S phase (referred to here as the S phase pathway). The former pathway depends on, among other genes, *RAD9*; the latter pathway depends on several genes involved in DNA replication; and both of these pathways depend on *MEC1* (Figure 1). This article describes the identification of another gene involved in the S phase pathway.

The mutations known to affect specifically the S phase pathway were identified by examining mutant alleles of genes known to be involved in replication or metabolism of DNA and by carrying out genetic screens. The designs of these screens, given current understanding of this field, are not expected to limit the genes thus identified to components of the S phase pathway. A more restrictive screen, *i.e.*, a screen for mutants defective specifically in the S phase pathway, should be a more efficient way to identify genes involved in that pathway. Such a screen is described in this article. It was based on the observation that cells missing only the cell cycle-wide pathway or only the S phase pathway are more proficient than *mec1* mutants in DNA damage responses, while cells missing both pathways are approximately as deficient as *mec1* mutants (Navas *et al.* 1996). Thus, in a strain carrying a temperature-sensitive allele of *RAD9*, mutants were isolated that, specifically at the restrictive temperature, showed not the moderate MMS sensitivity of a *rad9* mutant but instead the extreme MMS sensitivity of a *mec1* mutant. A secondary screen, requiring that the *rad9 geneX* double mutant be unable to slow replication in response to MMS at the restrictive temperature, was included to ensure that mutants were defective in a response that must occur during S phase. The screen yielded a mutant in a gene called *TOF1*.

TOF1 (*TO*poisomerase 1-associated *F*actor *1*) was previously identified in a two-hybrid screen for proteins that interact with the topoisomerase Top1p; the two proteins also interact *in vitro* (Park and Sternglanz 1999). Deletion of *TOF1* causes no obvious phenotype (Park and Sternglanz 1999). *TOF1* is 3.7 kb in length and its transcript peaks just before S phase (Cho *et al.* 1998; Spellman *et al.* 1998). The *Schizosaccharomyces pombe TOF1* homolog, *swi1*$^+$, is involved in mating-type switching (Egel *et al.* 1984); the other known *TOF1* homologs, which are found in *Aspergillus nidulans* and *Candida albicans*, have not been characterized.

In this article, cellular responses to abuse to DNA [by agents such as those used here, namely methyl methanesulfonate (MMS), UV, the *cdc13-1* mutation, and hydroxyurea (HU)] are referred to as genotoxic stress responses. A subset of these responses fit the original

Address for correspondence: Eric J. Foss, Division of Basic Sciences, A3-023, Fred Hutchinson Cancer Research Center, 1100 Fairview Ave. N., Seattle, WA 98109-1024. E-mail: efoss@fred.fhcrc.org

definition of checkpoint responses (Hartwell and Weinert 1989). MMS alkylates DNA (reviewed in Friedberg *et al.* 1995), resulting in DNA double-strand breaks (Chlebowicz and Jachymczyk 1979). UV induces pyrimidine dimers (reviewed in Friedberg *et al.* 1995). Cdc13p maintains telomeres both by protecting chromosome ends and by loading telomerase onto those ends (Nugent *et al.* 1996). *cdc13-1* mutants at restrictive temperature accumulate single-stranded DNA at their telomeres (Garvik *et al.* 1995). All lesions induced by the above three treatments are referred to as "DNA damage." HU inhibits ribonucleotide reductase, slowing or stopping DNA synthesis. Since HU is not known to directly damage DNA, this treatment is described here simply as "HU-induced stress."

MATERIALS AND METHODS

Yeast strains: All strains are in the A364a genetic background. Genotypes are listed in Table 1.

Mutant screen: A strain carrying a temperature-sensitive allele of *RAD9* (isolated by Mandy Paulovich; Whitehead Institute, Massachusetts Institute of Technology, Cambridge, MA) was EMS-mutagenized to 30% survival, and mutagenized cells were allowed to grow up into colonies on rich medium at restrictive temperature (37°). A total of 10,000 colonies were patched out on rich plates and replica plated to 0.008% MMS, which allows growth of *rad9* mutants but not *mec1 sml1* mutants. Duplicate MMS plates were incubated for three days at permissive (23°) and nonpermissive temperatures and scored for temperature-sensitive MMS sensitivity. The ~200 candidates scored as sensitive in two separate experiments were transformed with wild-type *RAD9* on a plasmid and with the vector alone. In 26 cases, wild-type *RAD9* suppressed the MMS sensi-

TABLE 1

Yeast strains

Strain	Genotype
YEF616	*MAT***a** *leu2 trp1 ura3 his3*
YEF620	*MAT***a** *leu2 trp1 ura3 his3*
YEF624	*MAT***a** *leu2 trp1 ura3 his3*
YEF628	*MAT***a** *leu2 trp1 ura3 his3*
YEF1115	*MAT***a** *leu2 trp1 ura3 his3*
YEF1116	*MAT***a** *leu2 trp1 ura3 his3*
YEF617	*MAT***a** *leu2 trp1 ura3 his3 rad9::LEU2*
YEF621	*MAT***a** *leu2 trp1 ura3 his3 rad9::LEU2*
YEF625	*MAT***a** *leu2 trp1 ura3 his3 rad9::LEU2*
YEF980	*MAT***a** *leu2 trp1 ura3 his3 rad9-*Δ*::Kan*^{r}
YEF981	*MAT***a** *leu2 trp1 ura3 his3 rad9-*Δ*::Kan*^{r}
YEF1117	*MAT***a** *leu2 trp1 ura3 his3 rad9-*Δ*::Kan*^{r}
YEF1112	*MAT***a** *leu2 trp1 ura3 his3 tof1-*Δ*::TRP1*
YEF1113	*MAT***a** *leu2 trp1 ura3 his3 tof1-*Δ*::TRP1*
YEF1114	*MAT***a** *leu2 trp1 ura3 his3 tof1-*Δ*::TRP1*
YEF1083	*MAT***a** *leu2 trp1 ura3 his3 rad9-*Δ*::Kan*^{r} *tof1-*Δ*::TRP1*
YEF1084	*MAT***a** *leu2 trp1 ura3 his3 rad9-*Δ*::Kan*^{r} *tof1-*Δ*::TRP1*
YEF1085	*MAT***a** *leu2 trp1 ura3 his3 rad9-*Δ*::Kan*^{r} *tof1-*Δ*::TRP1*
YEF569	*MAT***a** *leu2 trp1 ura3 his3 sml1-1 mec1-*Δ*::TRP1*
YEF672	*MAT***a** *leu2 trp1 ura3 his3 sml1-1 mec1-*Δ*::TRP1*
YEF674	*MAT***a** *leu2 trp1 ura3 his3 sml1-1 mec1-*Δ*::TRP1*
YEF1063	*MAT***a** *leu2 trp1 ura3 his3 sml1-*Δ*::Kan*^{r} *mec1-*Δ*::TRP1*
YEF1064	*MAT***a** *leu2 trp1 ura3 his3 sml1-*Δ*::Kan*^{r} *mec1-*Δ*::TRP1*
YEF1163	*MAT***a** *leu2 trp1 ura3 his3 cdc13-1*
YEF1164	*MAT***a** *leu2 trp1 ura3 his3 cdc13-1*
YEF1165	*MAT***a** *leu2 trp1 ura3 his3 cdc13-1*
YEF1172	*MAT***a** *leu2 trp1 ura3 his3 rad9-*Δ*::Kan*^{r} *cdc13-1*
YEF1173	*MAT***a** *leu2 trp1 ura3 his3 rad9-*Δ*::Kan*^{r} *cdc13-1*
YEF1174	*MAT***a** *leu2 trp1 ura3 his3 rad9-*Δ*::Kan*^{r} *cdc13-1*
YEF1181	*MAT***a** *leu2 trp1 ura3 his3 tof1-*Δ*::TRP1 cdc13-1*
YEF1182	*MAT***a** *leu2 trp1 ura3 his3 tof1-*Δ*::TRP1 cdc13-1*
YEF1183	*MAT***a** *leu2 trp1 ura3 his3 tof1-*Δ*::TRP1 cdc13-1*
YEF1190	*MAT***a** *leu2 trp1 ura3 his3 rad9-*Δ*::Kan*^{r} *tof1-*Δ*::TRP1 cdc13-1*
YEF1191	*MAT***a** *leu2 trp1 ura3 his3 rad9-*Δ*::Kan*^{r} *tof1-*Δ*::TRP1 cdc13-1*
YEF1192	*MAT***a** *leu2 trp1 ura3 his3 rad9-*Δ*::Kan*^{r} *tof1-*Δ*::TRP1 cdc13-1*
YEF1364	*MAT***a** *leu2 trp1 ura3 his3 RAD53-*$(HA)_2(HIS)_6$*::URA3*
YEF1365	*MAT***a** *leu2 trp1 ura3 his3 RAD53-*$(HA)_2(HIS)_6$*::URA3 rad9-*Δ*::Kan*^{r}
YEF1366	*MAT***a** *leu2 trp1 ura3 his3 RAD53-*$(HA)_2(HIS)_6$*::URA3 tof1-*Δ*::TRP1*
YEF1367	*MAT***a** *leu2 trp1 ura3 his3 RAD53-*$(HA)_2(HIS)_6$*::URA3 rad9-*Δ*::Kan*^{r} *tof1-*Δ*::TRP1*
YEF1368	*MAT***a** *leu2 trp1 ura3 his3 RAD53-*$(HA)_2(HIS)_6$*::URA3 sml1-*Δ*::Kan*^{r} *mec1-*Δ*::TRP1*

tivity of the candidate (*geneX*) at restrictive temperature. One of the 26 *rad9 geneX* double mutants was completely unable to slow S phase in MMS, as determined by flow cytometric analysis of cells grown in 0.033% MMS at 37°.

Identifying the gene: Attempts to clone *geneX* by complementing the HU sensitivity of *rad9 geneX* double mutants and *rad9 rad17 geneX* triple mutants by transformation with six different genomic libraries yielded only plasmids that carried *RAD9* as a strong suppressor of the HU sensitivity (in the former case) and *RAD24* as a weak high copy suppressor of the HU sensitivity (data not shown). The failure to recover a plasmid containing *TOF1* is probably due to the fact that *TOF1* is toxic to *Escherichia coli* (see below). Deletion of *RAD9* in variously marked strains allowed assembly of a collection of *rad9*-homozygous *geneX*-heterozygous diploids. These diploids were sporulated and dissected with hopes of detecting linkage between a marker and *geneX*, whose location was inferred from HU sensitivity that segregated 2:2. In one experiment, 29 out of 30 tetrads showed parental ditype segregation of HU sensitivity and *MET2*. Among the nearby genes, *TOF1* stood out because of its pre-S phase transcription induction (Cho *et al.* 1998; Spellman *et al.* 1998) and its association with Top1p (Park and Sternglanz 1999). Transformation of *rad9 geneX* double mutants with a PCR fragment containing only wild-type *TOF1*, followed by a long (overnight) outgrowth in rich medium to allow time for integration of the fragment (presumably at *tof1*) and expression of the wild-type protein, suppressed the HU sensitivity of the double mutant. Sequencing both strands of a PCR fragment containing "*tof1-1*" revealed a stop codon <6% from the translation start site that was absent in the wild-type control (amino acid 72, TRP, TGG changed to stop, TAG).

Efforts to subclone PCR fragments containing *TOF1* into a vector marked with *URA3* were unsuccessful, suggesting that *TOF1* is toxic to *E. coli*. To test this idea, equal amounts of this subcloning ligation mix were transformed into *E. coli*, selecting for β-lactamase (amp), and into *rad9*, "*tof1-1*," *ura3* yeast cells, selecting for *URA3*. The *E. coli* transformations yielded few colonies, none of which contained plasmids carrying *TOF1*. The yeast transformations yielded large numbers of colonies, most of which carried plasmids containing *TOF1*, as inferred from the transformants' loss of HU sensitivity. Furthermore, the HU resistance was plasmid dependent, as demonstrated by forcing loss of the plasmid on 5-fluoroorotic acid, which selects against *URA3*. Attempts to transfer these plasmids back into *E. coli* were unsuccessful, again suggesting that *TOF1* is toxic to *E. coli*. To further test this idea, equal amounts of DNA from yeast strains with plasmid-borne *TOF1* were cut separately with *Hin*dIII and *Kpn*I. Both of these enzymes cut within and outside of the *TOF1* open reading frame, thereby removing most of *TOF1*. The cut DNAs were ligated at low concentrations, to encourage intramolecular ligation reactions. An equal aliquot was mock treated. All three reaction mixes were transformed into the same preparation of competent *E. coli* alluded to five sentences earlier. The two reaction mixes in which most of the *TOF1* open reading frame had been removed from the plasmid yielded confluent lawns of bacterial transformants, while the uncut control yielded none. All plasmids checked contained the expected structure. These plasmids were then used to make a plasmid (pEF380) that was used to delete 77% of the *TOF1* open reading frame.

Flow cytometry: Three-milliliter samples for flow cytometry were pelleted, resuspended in 70% ethanol, washed with water, treated with 500 μl of 2 mg/ml RNaseA in 50 mm Tris, pH 7.5 for 1 hr at 37°, pelleted, treated with 500 μl of 2 mg/ml proteinase K in 50 mm Tris, pH 7.5 for 1 hr at 50°, pelleted, and stained with 1 μm Sytox green (Molecular Probes, Eugene, OR; product no. S-7020). Coefficients of variation (a measure of peak definition) are better for cells stained with Sytox than for cells stained with propidium iodide; consequently Sytox has been used in flow cytometric analysis of mammalian (Molecular Probes web site http://www.probes.com/handbook/figures/1512.html) and fission yeast cells (Rhind and Russell 1998). Conditions for using Sytox in flow cytometric analysis of *Saccharomyces cerevisiae* were determined by S. B. Haase (The Scripps Research Institute, La Jolla, California; personal communication). For a general discussion of flow cytometry in *S. cerevisiae*, see Haase and Lew (1997).

Viability curves: For the MMS and HU viability curves, cultures were grown overnight at 30° to mid-log phase (1.0×10^6–1.0×10^7 cells/ml), sonicated, counted in a Coulter Counter, spun down, and resuspended in fresh medium containing either 0.033% MMS or 200 mm HU. Aliquots were withdrawn at 0, 1, 2, 3, and 4 hr, sonicated, counted, diluted, and plated on synthetic complete medium. For the UV survival curve, cultures were grown, sonicated, and counted as above. Cells were then plated on synthetic complete medium and exposed to various UV doses (~260 nm; UVP model UVS-28; Upland, CA) on a rotating platform. The UV source was always turned on at least 30 min before use, and UV fluence was measured immediately before each experiment. In all three cases, plates were incubated at 30° for 3 days and every macroscopic colony was counted. Graphs show the percentage of cells that formed macroscopic colonies. Each data point represents the average of three different strains. Horizontal lines showing standard deviations are included in each case, except when their inclusion would obscure the data point to which they are relevant.

Staining spindles and DNA: Cultures were grown overnight at 30° to mid-log phase (1.0×10^6–1.0×10^7 cells/ml), sonicated, counted in a Coulter Counter, spun down, and resuspended in fresh medium containing 5 μm α-factor. After 2.5 hr at 30°, cells were spun down and resuspended in fresh medium containing 200 mm HU and 1 mg/ml pronase. After 3 more hours at 30°, cells were fixed with a 1:6 dilution of 37% formaldehyde, treated with Zymolyase and then with

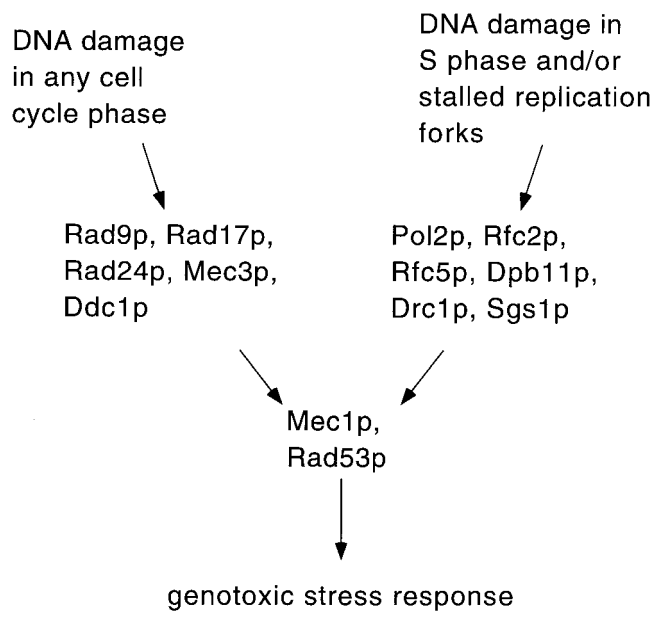

Figure 1.—A model for two parallel sensory pathways. The *RAD9*-dependent pathway functions throughout the cell cycle and detects DNA damage. The S phase-specific pathway detects both stalled replication forks and DNA damage.

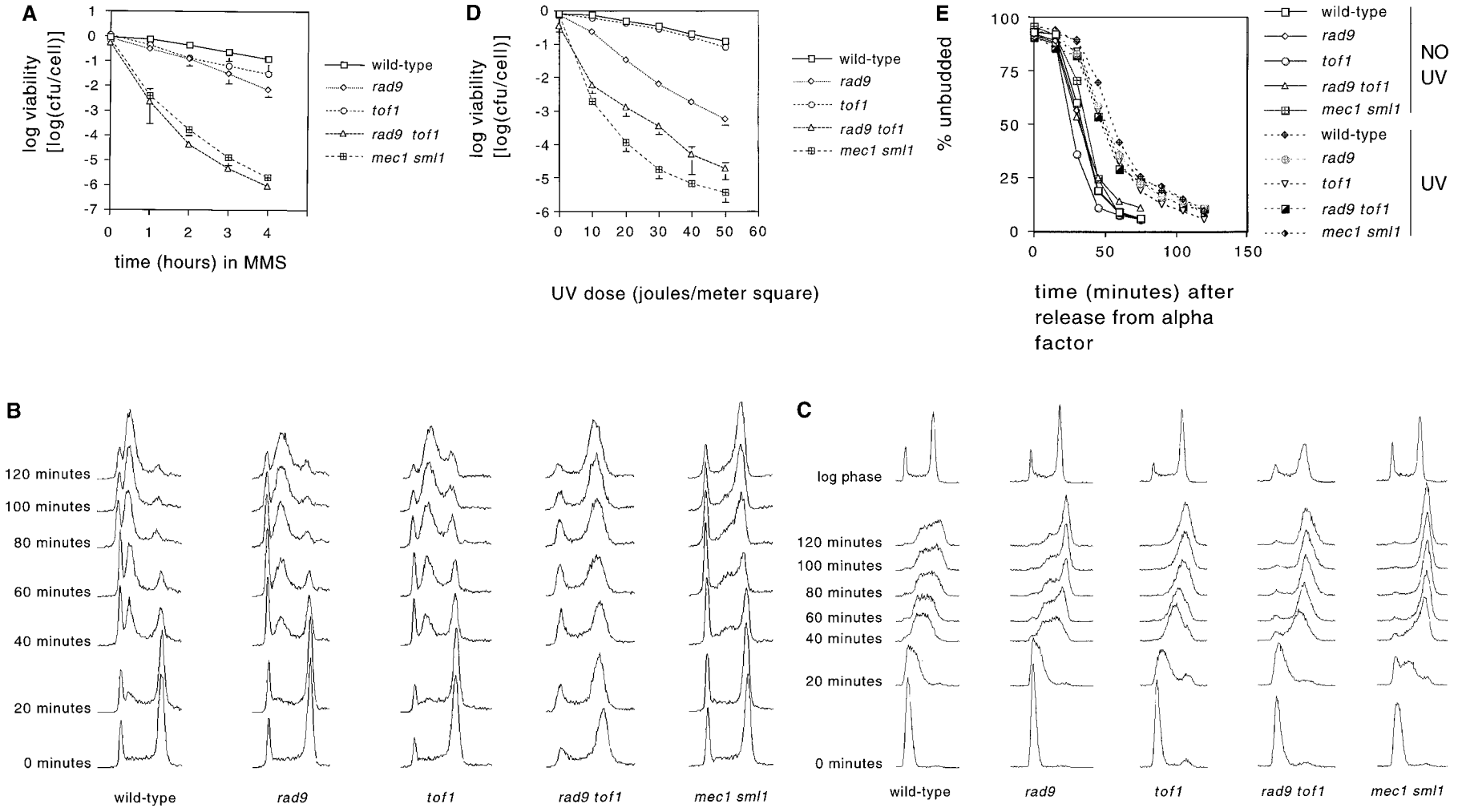
A
log viability [log(cfu/cell)]
time (hours) in MMS
wild-type
rad9
tof1
rad9 tof1
mec1 sml1
D
log viability [log(cfu/cell)]
UV dose (joules/meter square)
wild-type
rad9
tof1
rad9 tof1
mec1 sml1
E
% unbudded
time (minutes) after release from alpha factor
NO UV
UV
wild-type
rad9
tof1
rad9 tof1
mec1 sml1
B
120 minutes
100 minutes
80 minutes
60 minutes
40 minutes
20 minutes
0 minutes
wild-type
rad9
tof1
rad9 tof1
mec1 sml1
C
log phase
120 minutes
100 minutes
80 minutes
60 minutes
40 minutes
20 minutes
0 minutes
wild-type
rad9
tof1
rad9 tof1
mec1 sml1

rat anti-tubulin antibody (YOL1/34), and stained with FITC-conjugated goat anti-rat IgG and 4′,6-diamidino-2-phenylindole (DAPI). Samples were viewed with a Delta Vision microscope. All photos are shown at the same magnification.

***RNR3* transcription:** Cultures (25 ml) were grown overnight at 30° to mid-log phase (1.0×10^6–1.0×10^7 cells/ml), sonicated, and counted in a Coulter Counter; 1.5 ml was then removed and processed for flow cytometric analysis. The remainder of the culture was divided in two and spun down; one half ("G1" half) was resuspended in 10 ml of fresh medium containing 5 μM α-factor and incubated for 2 hr at 30° while the other half ("log phase" half) was resuspended in 10 ml of water. One-half of the log phase half (log phase-UV quarter) was transferred to an empty plastic petri dish and exposed to 50 J/m^2 UV (~260 nm; UVP model UVS-28) on a shaking platform. The UV source was always turned on at least 30 min before use, and UV fluence was measured immediately before each experiment. The log phase-UV quarter and the log phase-no UV quarter were then spun down, resuspended in 10 ml of fresh medium, and incubated for 30 min at 30° to allow time for induction of *RNR3* transcription (Navas *et al.* 1996). Cells were then transferred to 40-ml tubes containing crushed ice, pelleted at 4°, washed with 1 ml of cold TE, pelleted, frozen on dry ice, and stored at −70°. After the 2-hr incubation in α-factor, a 1.5-ml sample of the α-factor-arrested culture was removed for flow cytometric analysis and the remainder was treated as was the first half of the culture, except that the final 30-min outgrowth was in fresh medium that contained 5 μM α-factor. RNA was isolated and analyzed on a Northern blot. The probes used were the *Pvu*II (179) to *Hin*dIII (2585) fragment of *RNR3* and the entire open reading frame (though no more) of *PDA1*. The blot was stripped between the two probings. *PDA1*, which encodes pyruvate dehydrogenase, was used as a loading control because *PDA1* transcript levels are unaffected by a wide variety of treatments (Wenzel *et al.* 1995). Radioactive blots were quantified using a PhosphorImager. Data points represent levels of [(postirradiation *RNR3* transcript/postirradiation *PDA1* transcript)/(preirradiation *RNR3* transcript/preirradiation *PDA1* transcript)]. Each bar represents the average value for three different strains. Horizontal lines showing standard deviations are included in each case, but are indistinguishable from the top of the bar in the case of log phase *mec1 sml1*.

Cell body counts in *cdc13-1* strains: Cultures were grown overnight to mid-log phase (2×10^6–1×10^7) at 23°, sonicated, placed on a thin slab of rich agar on a microscope slide, covered with a slip and sealed with Vaseline. Cell proliferation at 37° was monitored by time-lapse video microscopy. Videotapes were later viewed to count the number of cell bodies at 0 and 6 hr. The graph in Figure 3B shows (number of cell bodies at 6 hr)/(number of cell bodies at 0 hr). Each bar represents the average from three different strains. Horizontal lines showing standard deviations are included in each case, but are indistinguishable from the top of the bar in the case of *tof1*.

Budding measurements: Cultures were grown to mid-log phase (1.0×10^6–1.0×10^7 cells per milliliter), pelleted, sonicated, and resuspended in medium with α-factor. After 2.5 hr in α-factor, cells were pelleted, sonicated, resuspended in water, and half of the culture was exposed to 50 J/m^2 UV, as described above. Cells were then pelleted and resuspended in fresh medium containing 1 mg/ml pronase. Samples were removed every 15 min, and multiple fields of cells were videotaped through a microscope. Videotapes were later viewed to quantify bud emergence. Horizontal lines showing standard deviations were deleted from this graph for clarity.

Protein preparation and Western blot analysis (Tyers *et al.* 1992; Emili *et al.* 1998) was performed as described previously.

RESULTS

Screen for mutants in the S phase pathway: A mutant screen to identify components of the S phase pathway was based on the assumption that mutants missing this pathway would be particularly dependent on the cell cycle-wide pathway, and therefore on *RAD9*, for surviving DNA damage (see Introduction and Figure 1). Thus, a strain carrying a temperature-sensitive allele of *RAD9* was EMS-mutagenized, 10,000 colonies were patched out, and mutants were isolated that showed extreme (*mec1*-like) MMS sensitivity specifically at the restrictive temperature. One of these *rad9 geneX* double mutants was completely unable to slow S phase in response to

Figure 2.—MMS and UV sensitivity, S phase slowing, and budding delay. (A) Viability in MMS. Mid-log phase overnight cultures were spun down and resuspended in fresh medium containing 0.033% MMS. Aliquots were withdrawn at 0, 1, 2, 3, and 4 hr, sonicated, counted, and plated on synthetic complete medium. Graph shows percentage of cells that formed macroscopic colonies after 3 days of incubation at 30°. Each genotype represents three different strains. cfu, colony-forming units. (B) MMS-induced slowing of S phase in asynchronous cultures. Mid-log phase overnight cultures were spun down and resuspended in fresh medium containing 0.033% MMS. Aliquots were withdrawn at 0, 20, 40, 60, 80, 100, and 120 min and processed for flow cytometry. Log phase *rad9 tof1* mutants produce wider peaks in flow cytometric analyses than do the other strains analyzed here. This may reflect a high rate of chromosome missegregation, which would be consistent with the low plating efficiency (colony-forming units per cell counted in a Coulter counter) observed in *rad9 tof1* double mutants (0.44 ± 0.14) as compared with wild-type (0.83 ± 0.06), *rad9* (0.82 ± 0.09), *tof1* (0.91 ± 0.17), and *mec1 sml1* (0.76 ± 0.13) strains. (C) MMS-induced slowing of S phase in synchronous cultures. Mid-log phase overnight cultures were spun down, α-factor-arrested for 2.5 hr, spun down, and resuspended in fresh medium containing 0.033% MMS and 1 mg/ml pronase. Aliquots were withdrawn from the overnight log phase culture (shown at front and back of each figure for reference) and at 20-min intervals from 0 to 120 min in MMS. (D) Viability after exposure to UV. Mid-log phase overnight cultures were spun down, resuspended in water, sonicated, counted, plated on synthetic complete medium, and exposed to various doses of UV irradiation (~260 nm from UVP model UVS-28). Graph shows percentage of cells that could form macroscopic colonies after 3 days of incubation at 30°. Each genotype represents the average of three different strains. (E) UV-induced delay in bud emergence. Overnight mid-log phase cultures were α-factor-arrested as above and allowed to resume growth in fresh medium at 30°. Aliquots were removed every 15 min, multiple fields of cells were videotaped through a microscope, and budding phenotypes were quantified later. The graph shows the percentage of unbudded cells. Error bars were removed because they cluttered the figure without altering the results. (Note that all irradiated cultures are indicated with dotted lines, while all unirradiated cultures are indicated with solid lines.)

MMS. The *geneX* phenotype was traced to a null mutation in *TOF1* (see MATERIALS AND METHODS). A deletion allele of *TOF1* was constructed for the experiments described below (see MATERIALS AND METHODS).

***TOF1* and *RAD9* have overlapping functions in response to MMS- and UV-induced damage:** Phenotypes exploited in the isolation of a *tof1* mutant are illustrated in Figure 2, A–C. Viability as a function of incubation time in 0.033% MMS is shown for *rad9* and *tof1* single mutants and for *rad9 tof1* double mutants, with wild-type and *mec1 sml1* strains serving as controls (Figure 2A). [All *mec1* strains used here carry a *sml1* mutation to suppress the lethality of the *mec1* mutation (ZHAO *et al.* 1998).] While the viabilities of *rad9* and *tof1* single mutants in MMS were only slightly lower than the viability of wild type, the *rad9 tof1* double mutant was as MMS sensitive as *mec1 sml1* (Figure 2A). The *rad9 tof1* double mutant also resembled the *mec1 sml1* mutant in being incapable of retarding S phase in response to MMS. This defect was apparent when log phase cultures were transferred into medium containing MMS (Figure 2B) as well as when cultures arrested in G1 with α-factor were allowed to resume proliferation in medium containing MMS (Figure 2C). The effect is easier to see in Figure 2B because all profiles contain cells in G1 and in G2/M, providing internal reference points, and because the time before the entire population has completed S phase is longer. (Cultures arrested in G1 acquire a G2 DNA content upon resumption of proliferation in less time than do log phase cultures; during a 2.5-hr α-factor block, newly formed daughter cells grow to the cell volume required for entrance into S phase.) Figure 2C is included to show that *rad9 tof1* double mutants do not simply arrest all cell cycle progression when shifted to MMS.

As shown in Figure 2D, deletion of *TOF1* increases the UV sensitivity of *rad9* mutants. For survival of wild-type cells in both MMS and UV, the data point to a greater role for *RAD9* than for *TOF1*, consistent with a cell cycle-wide function for *RAD9* and an S phase-specific function for *TOF1*.

Siede and colleagues reported that UV irradiation delays bud emergence and that this response is dependent on *RAD9* and *MEC1* (SIEDE *et al.* 1993, 1994, 1996). However, in the experiments reported here, mutation of neither *TOF1* nor any other genes tested affected this response (Figure 2E). This discrepancy may be due to strain background differences.

***TOF1* does not respond to UV- or *cdc13-1*-induced DNA damage outside of S phase:** If Tof1p functions specifically in the S phase pathway, its contribution to DNA damage response should be restricted to S phase. Thus, *TOF1* should contribute to UV-induced transcription of *RNR3* in log phase cultures, where a portion of the culture is in S phase, but not in cultures arrested in G1 with α-factor. (*RNR3* encodes a subunit of ribonucleotide reductase and is used here simply as a measure of UV-induced transcription.) Figure 3A shows *RNR3* transcript levels 30 min after cells were exposed to 50 J/m^2 UV irradiation. Consistent with previous results (NAVAS *et al.* 1996), wild-type cells showed higher *RNR3* transcript levels after UV-irradiation of both log phase and G1-arrested cultures, *rad9* mutants displayed higher *RNR3* transcript levels in log phase, but not G1, and *mec1 sml1* mutants did so in neither log phase nor G1 (Figure 3A). Consistent with *TOF1* function being restricted to S phase, *TOF1*'s contribution to UV-induced *RNR3* transcript levels was apparent in log phase cultures (compare *rad9* and *rad9 tof1*) but not in G1-arrested cultures (Figure 3A).

The *cdc13-1* mutation causes regions of single-stranded DNA to remain at telomeres in G2/M (GARVIK *et al.* 1995), and this induces a block to anaphase, which is reflected in a block to cytokinesis after S phase is complete (WEINERT and HARTWELL 1993). Thus, if *TOF1* function is restricted to S phase, it should not contribute to the block to cytokinesis. Figure 3B shows that *tof1* mutants were as proficient as wild-type cells in this response, while *rad9* mutants were deficient (as previously demonstrated; WEINERT and HARTWELL 1993). Instead of exacerbating the deficiency, deletion of *TOF1* in a *rad9* mutant appeared to partially restore the block to anaphase, but this result is likely to be an artifact of the low viability of *rad9 tof1 cdc13-1* triple mutants: even at 23°, viability, as measured by colony-forming units per cell, was only 49%, as opposed to about 75% for the other strains tested (Figure 3B).

***TOF1* and *RAD9* have overlapping functions in response to HU-induced stress:** As with MMS and UV, *tof1* and *rad9* caused synergistic sensitivity to HU (Figure 4A). [Although *tof1* mutants were highly viable in HU, they had a growth deficiency when streaked out on HU plates (data not shown).] Strains missing both *tof1* and *rad17*, *rad24*, or *mec3* were also HU sensitive, even though none of these single mutants appears more sensitive than wild-type when patches of cells are replica plated to 100 mM HU (data not shown). (*ddc1* was not tested.)

Cells exposed to HU phosphorylate Rad53p. This phosphorylation is controlled by *MEC1* and, to a lesser degree, *TEL1* (SANCHEZ *et al.* 1996). *RAD9* and *TOF1* were necessary and largely redundant for HU-induced phosphorylation of Rad53p (Figure 4B). The level of HU-induced phosphorylation in the *rad9 tof1* mutant was at least as low as in the *mec1 sml1* mutant and may be completely absent. Perhaps either Rad9p or Tof1p is absolutely required for a physical association of either Mec1p or Tel1p with Rad53p (see DISCUSSION). As seen previously (SANCHEZ *et al.* 1996; SUN *et al.* 1996), Rad53p protein accumulates in response to HU. This increase is only partially dependent on *MEC1*, *RAD9*, and *TOF1* (Figure 4B). The part of the increase not dependent on these genes may be a reflection of the MCB regulation of transcription of *RAD53*. (MCBs are promoter elements

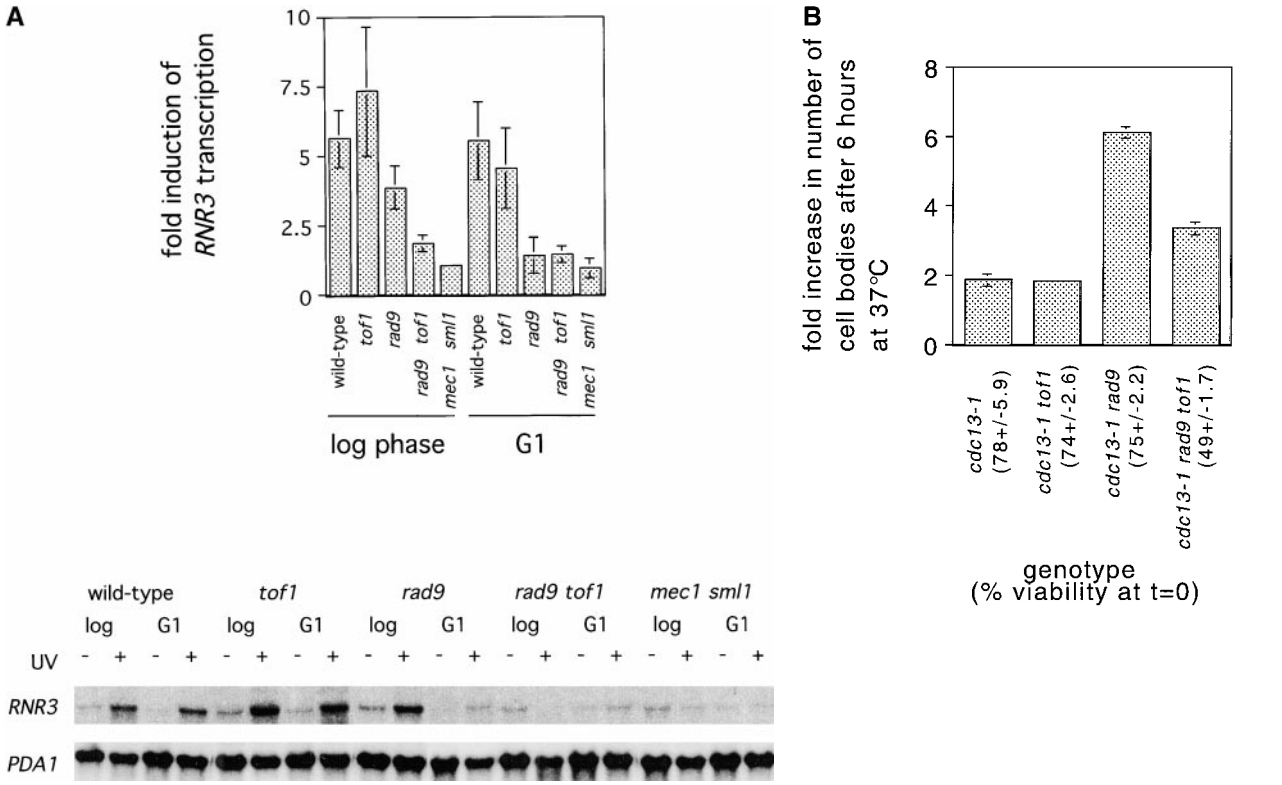

FIGURE 3.—UV-induced transcription and *cdc13-1*-induced anaphase delay. (A) UV-induced transcription of *RNR3*. Overnight mid-log phase cultures were split in two, half was exposed to 50 J/m^2 UV irradiation. The other half of the original culture was arrested in G1 (by incubation for 2 hr in α-factor) and then treated as was the first half of the original culture. Cells were then incubated for 30 min at 30° to allow time for induction of *RNR3* transcription. *PDA1* transcript levels were used as a loading control (WENZEL *et al.* 1995). Each bar represents the average (postirradiation *RNR3* transcript level/postirradiation *PDA1* transcript level)/(preirradiation *RNR3* transcript level/preirradiation *PDA1* transcript level) for three different strains. Aliquots were removed at each stage and processed for flow cytometry (data not shown). Representative RNAs are shown at the bottom. (B) *cdc13-1*-induced anaphase delay, as determined by measuring the delay in cytokinesis. Cultures were grown overnight at 23° to mid-log phase, sonicated, and spotted onto a thin slab of agarose on a microscope slide. Cell proliferation at 37° was followed using time-lapse video microscopy. Graph shows the number of cell bodies after 6 hr at 37° divided by the number of cell bodies at $t = 0$. Each genotype represents three different strains.

that cause transcription to peak in or just prior to S phase, and HU blocks cells in S phase.)

***tof1* mutants undergo concurrent S phase and spindle elongation in HU:** WEINERT *et al.* (1994) raised the possibility that the HU sensitivity of *mec1* mutants was due to their entry into anaphase, as inferred from spindle elongation, before DNA replication is complete. (Note, however, that spindle elongation need not reflect anaphase; SKIBBENS *et al.* 1999.) Consistent both with this idea and with the extreme HU sensitivity of *rad9 tof1* double mutants, *rad9 tof1* double mutants displayed elongated spindles in HU (Figure 4C). However, *tof1* single mutants also displayed some spindle elongation in HU (Figure 4C) prior to completion of S phase (Figure 4D). These data are consistent with the possibility that spindle elongation accounts for a small fraction of the HU-induced lethality of *rad9 tof1* and *mec1 sml1* mutants, but accounts for a large fraction of the HU-induced lethality of *tof1* mutants. Alternatively, the data could indicate that spindle elongation prior to completion of S phase is not lethal. A spindle elongation-independent role for *MEC1* in maintaining viability in HU is consistent with results reported by DESANY *et al.* (1998) that demonstrate a role for *MEC1* in maintaining viability in HU even when spindle elongation is chemically blocked. DAPI staining of the DNA in *mec1 sml1* and *rad9 tof1* mutants was uneven, suggesting DNA fragmentation, though this phenotype was subtle (data not shown). In contrast, the DNA in *tof1* mutants was indistinguishable from that in *rad9* mutants or wild-type cells (data not shown). The percentage of cells that showed obvious stretching of the DNA toward the spindle poles (<5%) was approximately the same in strains of all five genotypes (data not shown). I know of no simple model to explain why, despite numerous overlapping functions, *TOF1* and *RAD9* do not appear to overlap in their ability to block spindle elongation in HU.

DISCUSSION

This article provides evidence that *TOF1* is required for the *RAD9*-independent genotoxic stress response

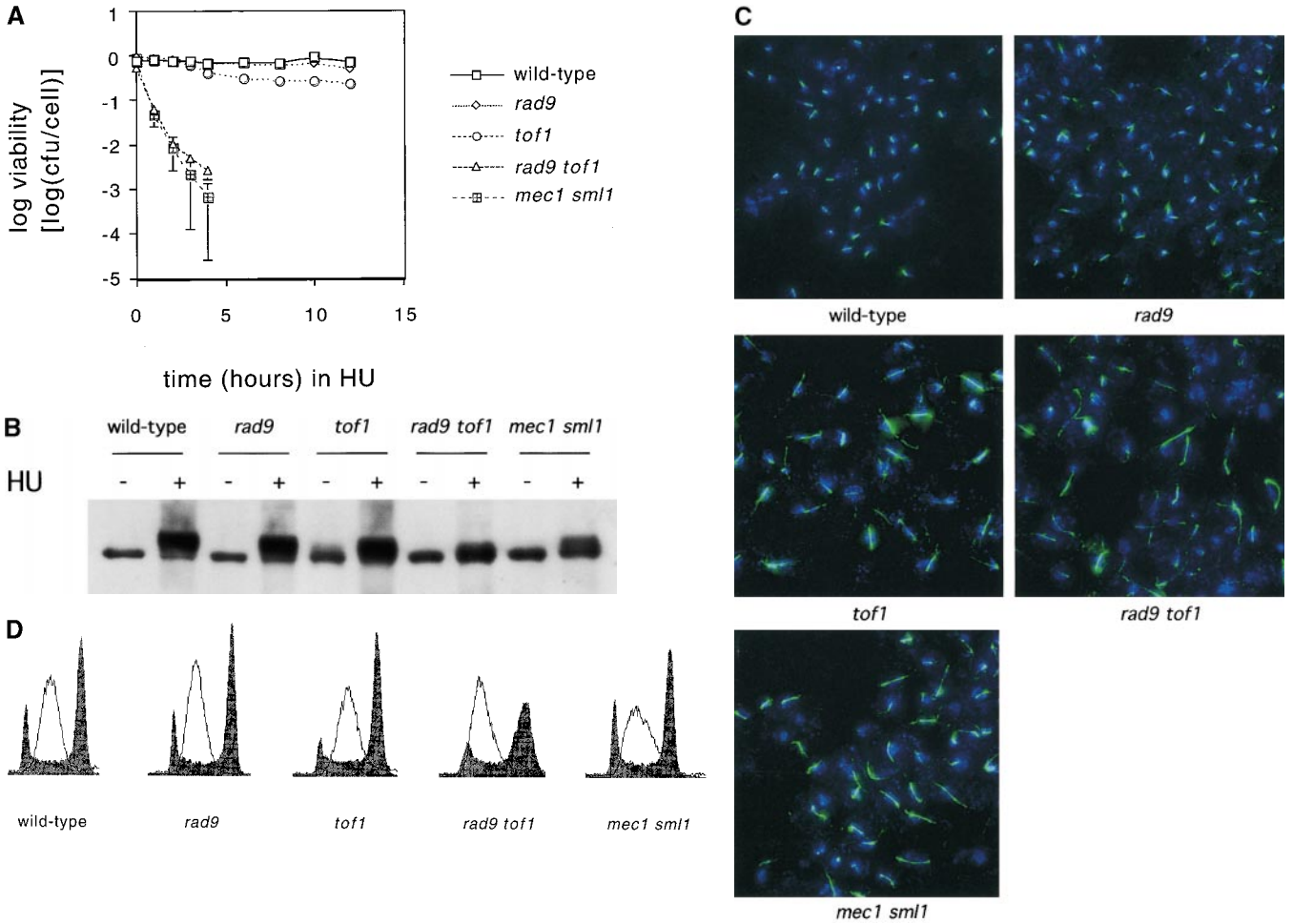

Figure 4.—Cellular responses to HU. (A) Viability in HU. Mid-log phase overnight cultures were spun down and resuspended in fresh medium containing 200 mM HU. Aliquots were withdrawn at 0, 1, 2, 3, and 4 hr and, for wild-type, *tof1*, and *rad9* strains, also at 6, 8, 10, and 12 hr, sonicated, counted, and plated on synthetic complete medium. Graph shows percentage of cells that could form macroscopic colonies after 3 days of incubation at 30°. In the *rad9 tof1* strains, HU treatment caused heterogeneous colony sizes, and many of the colonies were barely visible. Each genotype represents three different strains. (B) Phosphorylation of Rad53p in response to HU. Mobility of immunoprecipitated Rad53p tagged with HA was examined after late log phase cells were resuspended in fresh medium with or without 200 mM HU and grown for an additional 2 hr at 30°. (C) Spindle elongation in HU. Overnight mid-log phase cultures were α-factor-arrested, pelleted, and resuspended in fresh medium containing 200 mM HU and 1 mg/ml pronase. Aliquots were removed after 3 hr of incubation at 30°, fixed with formaldehyde, stained for DNA and spindles, and viewed under a Delta Vision microscope. All samples are shown at the same magnification, with spindles in green and DNA in blue. (D) Cell cycle position of strains 3 hr after release from an α-factor block into medium containing 200 mM HU. Shaded profiles of log phase cultures are shown for reference.

pathway that functions specifically within S phase: *tof1* and *rad9* showed synergistic sensitivity to MMS, UV, and HU, and the double mutant was unable to slow S phase in response to MMS and to phosphorylate Rad53p in response to HU. In log phase cultures, *tof1* and *rad9* showed synergistic inability to increase *RNR3* transcript levels in response to UV, but during G1 *TOF1* did not appear to contribute to this response. Mutation of *TOF1* did not impair the *cdc13-1*-induced delay in cytokinesis, which occurs in response to DNA damage present after S phase is complete.

The observations (1) that Top1p is the topoisomerase that relieves tension in replicating DNA (Kim and Wang 1989) and (2) that camptothecin, a chemical that covalently links Top1p to Top1p-cleaved DNA, causes strand breaks preferentially at replication forks in SV40, even when added after replication fork progression has been blocked by aphidicolin (Avemann *et al.* 1988), suggest that Top1p, and by implication Tof1p, functions at the replication fork. Thus the S phase specificity of *TOF1* function demonstrated in this article may reflect an association of Tof1p with the replication apparatus.

Previous work led to the belief that, while both the cell cycle-wide pathway and the S phase pathway were important for surviving DNA damage, only the S phase pathway was important for surviving replication blocks. In contrast, this work demonstrates that both pathways are important for survival in HU. [An earlier report

demonstrated a role for *RAD9* in allowing colony formation in the continuous presence of HU (Navas *et al.* 1996); however, blocking cell proliferation in the continuous presence of HU is not equivalent to HU-induced lethality (Allen *et al.* 1994).] If both pathways are capable of responding to DNA damage and to replication blocks, one is free to suppose both that they detect a common stress signal and that they use the same sensor protein to detect this signal.

Single-stranded DNA is a good candidate for a signal generated both by DNA damage and by stalled replication forks: The cell cycle-wide pathway responds to single-stranded DNA (Garvik *et al.* 1995). DNA lesions, such as double-strand breaks or thymine dimers, elicit a response from this pathway only if the lesions are processed to produce single-stranded DNA (Siede *et al.* 1994; Lydall *et al.* 1996). And aphidicolin, an agent that blocks DNA replication, generates single-stranded DNA in the SV40 replication system (Droge *et al.* 1985) and in melanoma cells (Lonn and Lonn 1988).

Mec1p is the obvious candidate for a protein that senses this single-stranded DNA: The mammalian *MEC1* homolog, DNA-PK, is a protein kinase that is activated by DNA double-strand ends (Smith and Jackson 1999). And the closest mammalian *MEC1* homolog, ATR, is a protein kinase whose activity can be stimulated by single-stranded DNA (Hall-Jackson *et al.* 1999). Thus, it is logical to suppose that single-stranded DNA constitutes a universal signal of genotoxic stress, and that Mec1p is a single-stranded DNA-dependent protein kinase that functions to detect this single-stranded DNA.

The functional redundancy between Rad9p and Tof1p demonstrated in this article may be an indication that these proteins have a common molecular activity. A function for Rad9p is suggested by the observation that DNA damage induces *MEC1*-dependent phosphorylation of Rad9p and that this allows Rad9p to bind Rad53p (Emili 1998; Sun *et al.* 1998); specifically, Rad9p may allow a lesion-dependent complex to form between Mec1p, Rad9p, and Rad53p. By analogy, Tof1p may allow a lesion-dependent complex to form between Mec1p, Tof1p, and Rad53p. As suggested above, Tof1p's S phase specificity may come from an association with the replication apparatus; thus, only when single-stranded DNA is generated at the replication fork (either from DNA damage or from a stalled DNA polymerase) would Mec1p act on Tof1p instead of on Rad9p to transmit the signal to Rad53p. The arguments in these last four paragraphs lead me to favor the model in Figure 5 over the more widely accepted model in Figure 1. These ideas are discussed extensively in Foss (2000).

An interaction between Tof1p and Top1p is not required for Tof1p function, since *top1* deletion mutants, unlike *tof1* deletion mutants, do not show synergistic HU sensitivity with *rad9* (data not shown). If the interaction between Tof1p and Top1p is functionally relevant, Top2p may be capable of fulfilling this function, as it is capable of fulfilling Top1p's role as a topoisomerase during DNA replication (Kim and Wang 1989). An obvious possibility for the function of a topoisomerase-Tof1p interaction is to link Tof1p to the replication apparatus.

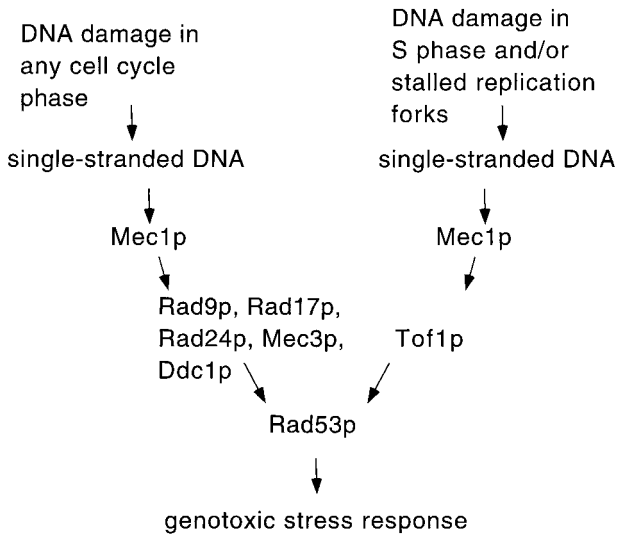

Figure 5.—Model in which Mec1p functions as a single-stranded DNA-dependent protein kinase at the top of both sensory pathways.

The phenotypes of *rad9 tof1* mutants are not always quantitatively equivalent to the phenotypes of *mec1 sml1* mutants. There are at least four reasons for expecting differences between strains of these two genotypes:

1. Deletion of *RAD9* does not eliminate the cell cycle-wide branch of the DNA damage response pathway; other genes in the pathway can make small contributions to DNA damage response in the absence of *RAD9* and vice versa (de la Torre Ruiz *et al.* 1998).
2. *RAD9* must have functions independent of *MEC1*, since deletion of *RAD9* in a *mec1* mutant leads to increased MMS sensitivity (Paulovich *et al.* 1997).
3. *MEC1* must have functions independent of *RAD9* and *TOF1*, since *MEC1* is an essential gene, while *rad9 tof1* mutants (and *rad9 rad24 tof1* mutants; data not shown) are viable.
4. The *MEC1* homolog *TEL1* can partially substitute for *MEC1*. [Deletion of *SML1* in a *rad9 tof1* mutant is not expected to eliminate differences in UV and HU sensitivity between *rad9 tof1* and *mec1 sml1* strains. If anything, it may slightly magnify the differences, since deletion of *SML1* causes a very slight decrease in UV, HU, and MMS sensitivity (Zhao *et al.* 1998).]

Four observations suggest that deletion of *TOF1* leads to increased endogenous DNA damage (three of which also suggest that the absence of *RAD9* leads to increased endogenous damage):

1. There was low-level phosphorylation of Rad53p in the absence of HU (Figure 4B).
2. The viability of *rad9 tof1* double mutants (0.44 ±

0.14) was lower than that of *rad9* mutants (0.82 ± 0.09; though the viability of *tof1* mutants was similar to that of wild-type cells).

3. The viability of *rad9 tof1 cdc13-1* mutants (0.49 ± 0.02) was lower than that of *rad9 cdc13-1* mutants (0.75 ± 0.02; though viability of *cdc13-1 tof1* mutants (0.74 ± 0.03) was similar to the viability of *cdc13-1* mutants (0.78 ± 0.06).
4. In the absence of any exogenous DNA-damaging agents, the flow cytometry profiles of log phase cultures of *rad9 tof1* mutants were wider than those of *rad9* mutants (though the profiles of wild-type cells and *tof1* mutants were similar).

Why might deletion of *TOF1* increase endogenous damage? Perhaps the replication fork is less stable in *tof1* mutants than in wild-type cells in the absence of exogenous genotoxic agents (an effect that need not be exaggerated by the presence of exogenous genotoxic agents). Clearly, other components of this pathway have functions besides detecting DNA structures generated by exogenous genotoxic agents, since both *MEC1* and *RAD53* are required for viability. Perhaps the presence of Mec1p, Rad53p, and Tof1p at replication forks helps to stabilize those forks when they stall during unperturbed S phases.

Does the observation that deletion of *TOF1* can cause endogenous DNA damage negate the idea that *TOF1* plays an active role in DNA damage response during S phase? No. The observation does not provide an explanation for *TOF1*'s role in UV-induced transcription of *RNR3* and in HU-induced phosphorylation of Rad53p (compare log phase *rad9* with log phase *rad9 tof1* in Figure 3A and compare *rad9* with *rad9 tof1* in Figure 4B). Furthermore, if deletion of *TOF1* was simply causing a higher level of endogenous damage, then the MMS, UV, and HU sensitivities of *rad9 tof1* double mutants should be approximately the same as that of *rad9* mutants; the absence of *TOF1* would just add a slightly higher baseline level of damage. This is not the case (Figures 2, A and D and 4A). Thus, as is likely the case with removal of *MEC1* or of *RAD53*, removal of *TOF1* creates endogenous damage; however, this does not belie its active role in genotoxic stress response.

I am enormously grateful to Jette Foss for many discussions critical to the intellectual development of this work and for extensive comments on this manuscript. In this regard, I also thank Toni Bedalov, Linda Breeden, Aida de la Cruz, Leon Dirick, Andrew Emili, Christian Frei, Barbara Garvik, Jim Haber, Lee Hartwell, Joe Horecka, Doug Koshland, Charles Laird, Andrew Murray, Patrick Paddison, Dina Raveh, Nick Rhind, Jim Roberts, Julia Sidorova, Frank Stahl, and David Toczyski. I thank Jeff Bachant, Andrew Emili, Elizabeth Greene, Steve Haase, Joe Horecka, and Tim Knight for advice on spindle staining, Western blots, sequence analysis, flow cytometry, Northern blots, and image analysis, respectively. I thank Scott Diede, Andrew Emili, and Mandy Paulovich for plasmids and strains. This work was supported by my fellowship from the Damon Runyon/Walter Winchell foundation and by Lee Hartwell's National Institutes of Health grant GM-11709.

LITERATURE CITED

Aboussekhra, A., J. E. Vialard, D. E. Morrison, M. A. de la Torre-Ruiz, L. Cernakova *et al.*, 1996 A novel role for the budding yeast *RAD9* checkpoint gene in DNA damage-dependent transcription. EMBO J. **15:** 3912–3922.

Allen, J. B., Z. Zhou, W. Siede, E. C. Friedberg and S. J. Elledge, 1994 The *SAD1/RAD53* protein kinase controls multiple checkpoints and DNA damage-induced transcription in yeast. Genes Dev. **8:** 2401–2415.

Avemann, K., R. Knippers, T. Koller and J. M. Sogo, 1988 Camptothecin, a specific inhibitor of type I DNA topoisomerase, induces DNA breakage at replication forks. Mol. Cell. Biol. **8:** 3026–3034.

Chlebowicz, E., and W. J. Jachymczyk, 1979 Repair of MMS-induced DNA double strand breaks in haploid cells of *Saccharomyces cerevisiae*, which requires the presence of a duplicate genome. Mol. Gen. Genet. **167:** 279–286.

Cho, R. J., M. J. Campbell, E. A. Winzeler, L. Steinmetz, A. Conway *et al.*, 1998 A genome-wide transcriptional analysis of the mitotic cell cycle. Mol. Cell **2:** 65–73.

de la Torre-Ruiz, M. A., C. M. Green and N. F. Lowndes, 1998 *RAD9* and *RAD24* define two additive, interacting branches of the DNA damage checkpoint pathway in budding yeast normally required for Rad53 modification and activation. EMBO J. **17:** 2687–2698.

Desany, B. A., A. A. Alcasabas, J. B. Bachant and S. J. Elledge, 1998 Recovery from DNA replicational stress is the essential function of the S-phase checkpoint pathway. Genes Dev. **12:** 2956–2970.

Droge, P., J. M. Sogo and H. Stahl, 1985 Inhibition of DNA synthesis by aphidicolin induces supercoiling in simian virus 40 replicative intermediates. EMBO J. **4:** 3241–3246.

Egel, R., D. H. Beach and A. J. Klar, 1984 Genes required for initiation and resolution steps of mating-type switching in fission yeast. Proc. Natl. Acad. Sci. USA **81:** 3481–3485.

Emili, A., 1998 *MEC1*-dependent phosphorylation of Rad9p in response to DNA damage. Mol. Cell **2:** 183–189.

Foss, E. J., 2000 Is Rad9p upstream or downstream of Mec1p? Cold Spring Harbor Symp. Quant. Biol. **65:** (in press).

Friedberg, E. C., G. C. Walker and W. Siede, 1995 *DNA Repair and Mutagenesis.* ASM Press, Washington, DC.

Garvik, B., M. Carson and L. Hartwell, 1995 Single-stranded DNA arising at telomeres in *cdc13* mutants may constitute a specific signal for the *RAD9* checkpoint. Mol. Cell. Biol. **15:** 6128–6138.

Haase, S. B., and D. J. Lew, 1997 Flow cytometric analysis of DNA content in budding yeast. Methods Enzymol. **283:** 322–332.

Hall-Jackson, C. A., D. A. Cross, N. Morrice and C. Smythe, 1999 ATR is a caffeine-sensitive, DNA-activated protein kinase with a substrate specificity distinct from DNA-PK. Oncogene **18:** 6707–6713.

Hartwell, L. H., and T. A. Weinert, 1989 Checkpoints: controls that ensure the order of cell cycle events. Science **246:** 629–634.

Kim, R. A., and J. C. Wang, 1989 Function of DNA topoisomerases as replication swivels in *Saccharomyces cerevisiae*. J. Mol. Biol. **208:** 257–267.

Kiser, G. L., and T. A. Weinert, 1996 Distinct roles of yeast *MEC* and *RAD* checkpoint genes in transcriptional induction after DNA damage and implications for function. Mol. Biol. Cell **7:** 703–718.

Longhese, M. P., V. Paciotti, R. Fraschini, R. Zaccarini, P. Plevani *et al.*, 1997 The novel DNA damage checkpoint protein Ddc1p is phosphorylated periodically during the cell cycle and in response to DNA damage in budding yeast. EMBO J. **16:** 5216–5226.

Lonn, U., and S. Lonn, 1988 Extensive regions of single-stranded DNA in aphidicolin-treated melanoma cells. Biochemistry **27:** 566–570.

Lydall, D., Y. Nikolsky, D. K. Bishop and T. Weinert, 1996 A meiotic recombination checkpoint controlled by mitotic checkpoint genes. Nature **383:** 840–843.

Navas, T. A., Y. Sanchez and S. J. Elledge, 1996 *RAD9* and DNA polymerase epsilon form parallel sensory branches for transducing the DNA damage checkpoint signal in *Saccharomyces cerevisiae*. Genes Dev. **10:** 2632–2643.

Nugent, C. I., T. R. Hughes, N. F. Lue and V. Lundblad, 1996 Cdc13p: a single-strand telomeric DNA-binding protein

with a dual role in yeast telomere maintenance. Science **274:** 249–252.

Park, H., and R. Sternglanz, 1999 Identification and characterization of the genes for two topoisomerase I-interacting proteins from *Saccharomyces cerevisiae*. Yeast **15:** 35–41.

Paulovich, A. G., and L. H. Hartwell, 1995 A checkpoint regulates the rate of progression through S phase in *S. cerevisiae* in response to DNA damage. Cell **82:** 841–847.

Paulovich, A. G., R. U. Margulies, B. M. Garvik and L. H. Hartwell, 1997 *RAD9*, *RAD17*, and *RAD24* are required for S phase regulation in *Saccharomyces cerevisiae* in response to DNA damage. Genetics **145:** 45–62.

Rhind, N., and P. Russell, 1998 The *Schizosaccharomyces pombe* S-phase checkpoint differentiates between different types of DNA damage. Genetics **149:** 1729–1737.

Sanchez, Y., B. A. Desany, W. J. Jones, Q. Liu, B. Wang *et al.*, 1996 Regulation of *RAD53* by the ATM-like kinases *MEC1* and *TEL1* in yeast cell cycle checkpoint pathways. Science **271:** 357–360.

Siede, W., A. S. Friedberg and E. C. Friedberg, 1993 *RAD9*-dependent G1 arrest defines a second checkpoint for damaged DNA in the cell cycle of *Saccharomyces cerevisiae*. Proc. Natl. Acad. Sci. USA **90:** 7985–7989.

Siede, W., A. S. Friedberg, I. Dianova and E. C. Friedberg, 1994 Characterization of G1 checkpoint control in the yeast *Saccharomyces cerevisiae* following exposure to DNA-damaging agents. Genetics **138:** 271–281.

Siede, W., J. B. Allen, S. J. Elledge and E. C. Friedberg, 1996 The *Saccharomyces cerevisiae MEC1* gene, which encodes a homolog of the human ATM gene product, is required for G1 arrest following radiation treatment. J. Bacteriol. **178:** 5841–5843.

Skibbens, R. V., L. B. Corson, D. Koshland and P. Hieter, 1999 Ctf7p is essential for sister chromatid cohesion and links mitotic chromosome structure to the DNA replication machinery. Genes Dev. **13:** 307–319.

Smith, G. C., and S. P. Jackson, 1999 The DNA-dependent protein kinase. Genes Dev. **13:** 916–934.

Spellman, P. T., G. Sherlock, M. Q. Zhang, V. R. Iyer, K. Anders *et al.*, 1998 Comprehensive identification of cell cycle-regulated genes of the yeast *Saccharomyces cerevisiae* by microarray hybridization. Mol. Biol. Cell **9:** 3273–3297.

Sun, Z., D. S. Fay, F. Marini, M. Foiani and D. F. Stern, 1996 Spk1/Rad53 is regulated by Mec1-dependent protein phosphorylation in DNA replication and damage checkpoint pathways. Genes Dev. **10:** 395–406.

Sun, Z., J. Hsiao, D. S. Fay and D. F. Stern, 1998 Rad53 FHA domain associated with phosphorylated Rad9 in the DNA damage checkpoint. Science **281:** 272–274.

Tyers, M., G. Tokiwa, R. Nash and B. Futcher, 1992 The Cln3-Cdc28 kinase complex of *S. cerevisiae* is regulated by proteolysis and phosphorylation. EMBO J. **11:** 1773–1784.

Weinert, T. A., and L. H. Hartwell, 1988 The *RAD9* gene controls the cell cycle response to DNA damage in *Saccharomyces cerevisiae*. Science **241:** 317–322.

Weinert, T. A., and L. H. Hartwell, 1993 Cell cycle arrest of *cdc* mutants and specificity of the *RAD9* checkpoint. Genetics **134:** 63–80.

Weinert, T. A., G. L. Kiser and L. H. Hartwell, 1994 Mitotic checkpoint genes in budding yeast and the dependence of mitosis on DNA replication and repair. Genes Dev. **8:** 652–665.

Wenzel, T. J., A. W. R. H. Teunissen and H. Y. Steensma, 1995 *PDA1* mRNA: a standard for quantitation of mRNA in *Saccharomyces cerevisiae* superior to *ACT1* mRNA. Nucleic Acids Res. **23:** 883–884.

Zhao, X., E. G. D. Muller and R. Rothstein, 1998 A suppressor of two essential checkpoint genes identifies a novel protein that negatively affects dNTP pools. Mol. Cell **2:** 1–20.

Zhou, Z., and S. J. Elledge, 1993 *DUN1* encodes a protein kinase that controls the DNA damage response in yeast. Cell **75:** 1119–1127.

Communicating editor: J. Rine